

Surface magnetic ordering in chromium

D. R. Grempel

Department of Physics, University of Pennsylvania, Philadelphia, Pennsylvania 19104

(Received 21 May 1981)

The magnetic properties of the (001) surface of chromium at finite temperature are investigated by means of spin-fluctuation theory. It is found that, in contrast with the behavior in the bulk, large localized magnetic moments form at the surface. Interactions between these moments and their coupling to bulk spin fluctuations are included in the calculations. The results show that magnetic ordering at the surface persists well above the bulk Néel temperature. Comparison is made with available experimental results.

I. INTRODUCTION

The effect of surfaces on the magnetic properties of transition metals has recently attracted increasing attention. Several authors¹⁻⁴ have indicated that significant changes in the magnetic properties may result from the sharp changes in the nature and properties of the electronic states at and near surfaces. In fact, there is now considerable experimental evidence to support these ideas.⁵⁻¹² Some experiments probe the change in the ground-state magnetic moment of surface atoms in ferromagnetic transition-metal crystals⁵⁻⁸ with results that are generally in good agreement with the predictions of detailed self-consistent band-structure calculations.^{13,14} Other experiments study the temperature dependence of the magnetic properties of paramagnetic materials. In particular, the magnetic susceptibility was measured for ultrafine particles of vanadium,⁹ thin films of transition metals¹⁰ and liquid ³He confined on different substrates.¹² It was found that the magnetic susceptibility of these systems exhibits a Curie-Weiss temperature dependence superimposed on the nearly constant contribution of the bulk. Such a temperature dependence is evidence of the formation of local magnetic moments. Their absence in the bulk suggests that local-moment formation has taken place at or near the surfaces. In a previous paper¹⁵ it has been shown that in the case of vanadium particular features of the surface electronic structure produce large, long-lived fluctuations of the surface local moment. These fluctuations give a surface contribution to the magnetic susceptibility that has the required temperature dependence. Related ideas have been used¹⁶ in the analysis of ³He experiments.

If local magnetic moments can appear at the surface of a paramagnetic material, the existence of a surface-ordered phase may be possible. Surfaces of transition metals are known to exhibit considerable anisotropy for spin rotations¹⁷ and quasi-two-

dimensional ordering can occur.

Chromium is particularly interesting in this context. It has recently been reported¹⁸ that small particles of bcc chromium exhibit a magnetically ordered phase up to temperatures well above the Néel temperature of bulk chromium. The dependence of the magnetization on particle size suggests that this is a surface effect. The existence of a ferromagnetic layer at the interface between chromium and MgF₂ at room temperature was observed in magnetoplasma wave absorption measurements.¹⁹ It has also been suggested on theoretical grounds that surface magnetism in chromium may persist above T_N .²⁰

In this paper the surface magnetic properties of chromium (001) are studied above and below T_N . This surface has been chosen because one expects to find more pronounced effects in this case. While the results reported here can not be directly applied to the polycrystalline samples used in the experiments, the qualitative conclusions should also apply in that case.

The basic ideas of this paper are the following. The Fermi level of chromium is in the deep valley between the bonding and antibonding d bands. As a result, the density of states at the Fermi level and the uniform field susceptibility are small. At the (001) surface band narrowing produces a large enhancement of the local spin susceptibility. This enhancement causes an instability against the formation of local moments. The interactions between these moments determine the stability of an ordered surface. These interactions are indirect, mediated by the itinerant electrons. In their motion the electrons sample the magnetization throughout the crystal. Thus, bulk polarization effects play a very important role. This is quite different from the situation reported earlier¹⁵ for vanadium where these effects were negligible.

The organization of this paper is as follows. The model Hamiltonian and its ground-state properties

are presented in Sec. II. Section III contains a discussion of spin-fluctuation effects and of the methods used in the calculations. The results of numerical calculations for chromium are presented in Sec. IV. This is followed by a summary and concluding remarks.

II. MODEL AND GROUND-STATE PROPERTIES

The electronic structure of (001) chromium is represented by a Hamiltonian that includes a local exchange interaction.²¹

$$H = H_0 - \frac{1}{4} \sum_i U_i S_{iz} S_{iz} \quad (1)$$

H_0 is the band Hamiltonian within the tight-binding representation. The second term on the right-hand side of Eq. (1) models the spin-dependent part of the electron-electron interaction. S_{iz} is the z component of the total electronic spin at site i and U_i is the exchange constant. Its value for surface atoms may be different from that in the bulk. Charge-rearrangement effects are included in H_0 by an appropriate choice of the one-electron potential. To take into account spin anisotropy only one component of the spin, along one of the easy axes, is considered.

The band Hamiltonian H_0 includes five d orbitals per site with nearest- and next-nearest-neighbor hopping terms.²² The effects of the s - p bands are not included because the main contribution to the density of states around the Fermi level comes from the d states. Following standard procedures²³ the hopping matrix elements were fixed at their bulk values throughout the system. The surface diagonal elements, however, were scaled in order to preserve charge neutrality.

Figure 1 shows the local bulk and surface densities of states (DOS) for the paramagnetic phase. They have been computed by the real-space continued-fraction expansion technique²⁴ including 16 exact moments of the density of states. The results are comparable to those of Ref. 22.

A large peak in the surface DOS near the Fermi energy is the most relevant feature in Fig. 1. It is characteristic of the electronic structure of the (001) surface of transition metals with the bcc structure. This peak appears in both model²⁵ and first-principles²⁶ calculations. Its relevance for the problem of surface spin fluctuations has been pointed out previously.¹⁵

At low temperature chromium orders in a spin-density-wave configuration. The nearly commensurate wave vector is along one of the fourfold symmetry axes. The ground-state spin polarization is of the form

$$S_z(\vec{x}) = S_0 \cos(\vec{Q} \cdot \vec{x}) \quad (2)$$

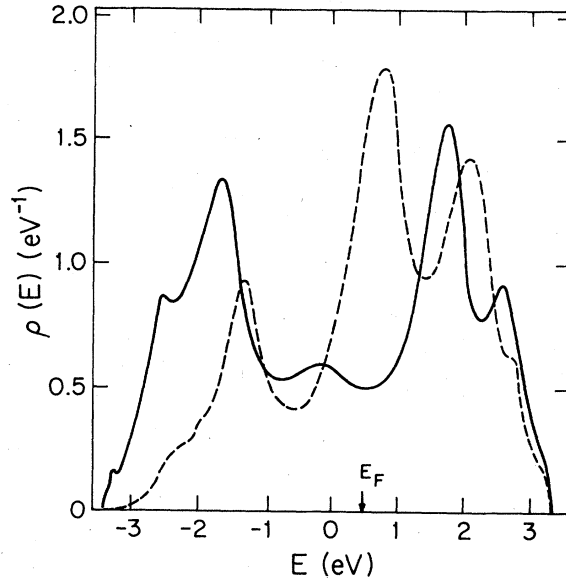


FIG. 1. Bulk (solid line) and (001) surface (dashed line) densities of states of chromium in the paramagnetic phase.

where $\vec{Q} = 2\pi/a(0, 0, 1 \pm \delta)$ and δ is small.^{27,28} The discommensuration plays no role in this problem and it has been neglected for simplicity. In the commensurate case electrons of different spins move in opposite oscillating potentials given by

$$V^\pm(x) = \mp g \cos(\vec{Q} \cdot \vec{x}) \quad (3)$$

Within the Hartree-Fock approximation the size of the antiferromagnetic gap g is self-consistently determined by the condition

$$2g = UM_s(g) \quad (4)$$

$M_s(g)$ is the equilibrium value of the staggered magnetization in the presence of the potential of Eq. (3) and U the bulk exchange constant.

For a semi-infinite crystal g is nonuniform. The simplest model to describe its variation consists of fixing it at its bulk value everywhere except at the surface where it takes a different value, g_s . The local gap at the surface is related to the surface magnetic moment by an equation similar to (4). This model is supported by a calculation by Allan,²⁹ who has shown, using perturbation theory, that the antiferromagnetic gap on layer l decays to the bulk value according to

$$g(l) - g_b \sim \exp\left(-\frac{l}{l_0}\right) \quad (5)$$

with $l_0 \sim 1.67$ in units of interplanar spacing.

Figure 2 shows the bulk and surface DOS for both spin directions in the antiferromagnetic state. The

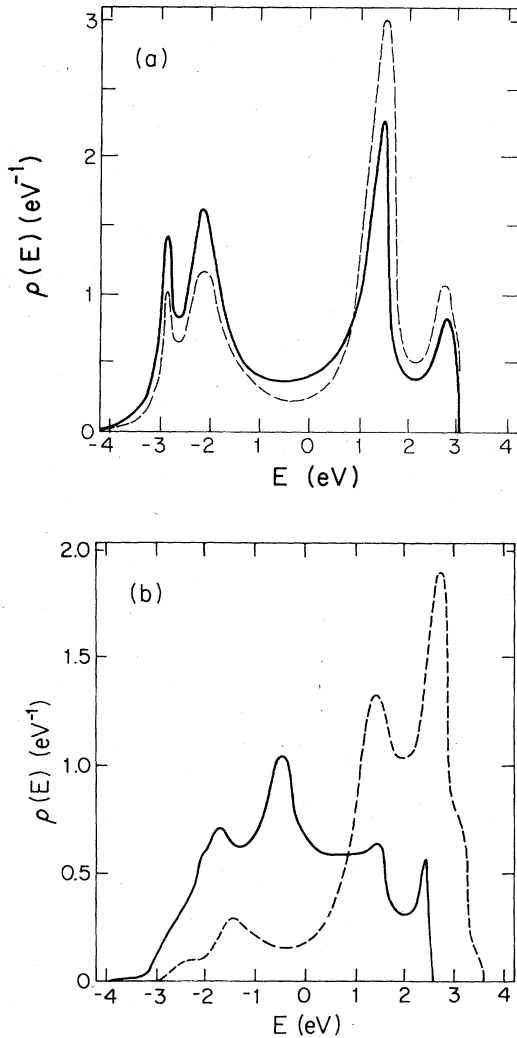


FIG. 2. (a) Bulk density of states in the antiferromagnetic ground state. Solid line: majority electrons. Dashed line: minority electrons. (b) Same as (a) but for the (001) surface.

exchange constant U was taken to be uniform throughout the system and its magnitude determined by a fit to the experimental value of the bulk magnetic moment ($0.6\mu_B$). Since the gap in the bulk is very small (~ 0.22 eV) the DOS for opposite spins are very similar. The gap at the surface is very large (0.95 eV) and, as a result, the surface magnetic moment is much larger ($2.6\mu_B$). The peaks in the den-

sities of states for different spins are considerably shifted from their positions in the paramagnetic phase. These results are in agreement with those of Ref. 22.

The marked differences between surface and bulk magnetic properties is a result of the drastic changes in the electronic properties that occur at a (001) surface. On other faces these changes are less pronounced and their effect on the surface magnetic properties smaller.

This mean-field procedure can be extended to finite temperatures very easily. Not surprisingly the results for the temperature dependence of the magnetization and susceptibility are wrong. This is because thermal fluctuations, neglected above, play a very important role in this problem.

III. FLUCTUATIONS

The calculation of the temperature dependence of the magnetic properties is most conveniently performed by formulating the problem directly in terms of spin-fluctuation collective variables.²¹ By the use of the Hubbard-Stratonovich transformation³⁰ the partition function of the system of interacting electrons is obtained by calculating the partition function of a system of noninteracting electrons moving in a random magnetic field with a Gaussian distribution. The result is then averaged over all possible field configurations. Explicitly, the partition function is given by³¹

$$Z = \int d[\xi] \exp \left\{ - \int_0^\beta d\tau \sum_i \xi_i^2(\tau) \right\} Z_0[\lambda\xi] , \quad (6)$$

where

$$Z_0[\lambda\xi] = Z_0[0] \left\langle T_\tau \exp \left[- \int_0^\beta d\tau \sum_i \xi_i(\tau) S_{iz}(\tau) \right] \right\rangle_0 . \quad (7)$$

The coupling constant $\lambda = (UkT)^{1/2}$ and $Z_0[0]$ is the partition function of noninteracting electrons in zero field. The functional integral in (6) extends over all possible functions $\xi_i(\tau)$. After representing Eq. (7) by a coupling-constant integration³¹ the partition function can be written as

$$Z = \int d[\xi] \exp(-H[\xi]) , \quad (8)$$

where the effective spin-fluctuation Hamiltonian H is given by

$$H[\xi] = \frac{1}{\beta} \int_0^\beta d\tau \left(\sum_i \xi_i^2(\tau) - \beta \sum_{i,m,s} s \int_0^\lambda d\lambda \xi_i(\tau) G_{im,im}^s(\tau, \tau^+, [\lambda\xi]) \right) . \quad (9)$$

$G_{im,jm'}^s(\tau, \tau^+, [\lambda\xi])$ is the Green's function of the electrons in the magnetic field $\xi_i(\tau)$, s is a spin label, and m, m' are orbital indices. All quantities of interest can be obtained from the correlation functions of the field ξ . The magnetization and susceptibility are given by³¹

$$M_i = \frac{2\lambda}{U} \langle \xi_i(\tau) \rangle \quad (10)$$

and

$$\chi_{ij} = \frac{2}{U} \left(\frac{2}{\beta} \int_0^\beta d\tau \langle \xi_i(\tau) \xi_j(0) \rangle - \delta_{ij} \right), \quad (11)$$

where the angular brackets denote the average of a functional of ξ

$$\langle A[\xi] \rangle = \frac{1}{Z} \int d[\xi] A[\xi] \exp(-H[\xi]) . \quad (12)$$

The evaluation of Eqs. (8) to (11) is considerably simplified by the use of the "static"³² and saddle-point³³ approximations. Neglecting the time dependence of $\xi_i(\tau)$, Eq. (9) is readily integrated to give

$$H[\xi] = \sum_i \xi_i^2 + \beta \int_{-\infty}^{\infty} \frac{dE}{\pi} \frac{1}{1 + \exp(\beta E)} \text{Im} \ln \text{Det}[1 - \bar{V}\bar{G}^0(E)] , \quad (13)$$

where the matrix elements $V_{im,jm'} = \mp \lambda \xi_i \delta_{ij} \delta_{mm'}$, and $G^0(E)$ is the Green's function corresponding to H_0 . In order to apply the saddle-point method, the configurations that minimize $H[\xi]$ must be found. This is easily done at very high temperature because fields at different sites decouple from each other.³² As a result Eq. (13) reduces to

$$H[\xi] = \beta \sum_i F(\Delta_i) , \quad (14)$$

where the local free energy is defined as

$$F(\Delta_i) = \frac{\Delta_i^2}{U} + \beta \int_{-\infty}^{\infty} \frac{dE}{\pi} \frac{1}{1 + \exp(\beta E)} \sum_{s,m} \text{Im} \ln[1 + s\Delta_i G_{im,im}^0(E)] \quad (15)$$

and $\Delta_i = \lambda \xi_i$. Figure 3 shows $F(\Delta)$ for sites in the bulk and at the (001) surface of chromium. The local free energy has a minimum at $\Delta = 0$ in the bulk whereas it has two deep minima at the surface. The condition for the appearance of two minima is $U\chi_i^0 > 1$ where $2\chi_i^0$ is the local spin susceptibility. Since χ_i^0 is very large for a surface atom, this condition is satisfied at the surface. Away from the minima, the local free energy increases rapidly. It follows that in the configurations that give the largest contribution to the free energy the local field in the bulk fluctuates with small amplitude around $\xi = 0$. In contrast, at the surface, it takes the values $\pm \bar{\xi}$ at which the local minima occur. The surface local fields are thus of large amplitude.

At finite temperatures intersite coupling must be taken into account. In the paramagnetic phase, the qualitative features of the saddle-point configurations remain the same as above. When the system orders, ξ_i has a nonvanishing average value. The bulk low-lying excitations become small oscillations about the displaced equilibrium value. At the surface, the minima of the local free energy are no longer equivalent. It will turn out that, in the bulk, the fluctuations are localized in \vec{k} space in two narrow regions around the origin and the edge of the Brillouin zone. In contrast, at the surface, fluctuations retain a local character in real space. The coupling between the two

arises mainly from the polarization of the bulk produced by a nonzero surface magnetization. The inclusion of the polarization effect requires the evaluation of the temperature-dependent nonlocal bulk spin susceptibility.

Because they are of different nature, bulk and

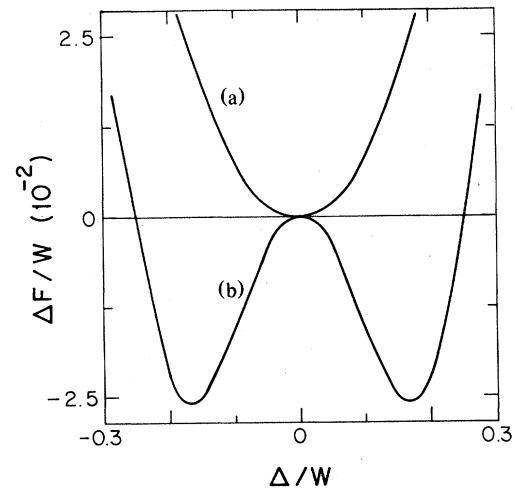


FIG. 3. Local free energy as a function of the local band splitting at high temperatures, for (a) bulk and (b) surface atoms. The energies are in units of the bandwidth (7 eV).

surface-fluctuation effects must be treated separately. This is done in the next two subsections.

A. Bulk fluctuations

Expanding the effective Hamiltonian (13) in powers of ξ one obtains in the paramagnetic phase³¹

$$H[\xi] = \sum_q v_2(\vec{q}) \vec{q} \xi(-\vec{q}) + \sum_n v_{2n}(\vec{q}_1, \dots, \vec{q}_{2n}) \xi(\vec{q}_1) \cdots \xi(\vec{q}_{2n}) . \tag{16}$$

The vertices $v_{2n}(q)$ are given in terms of traces of products of Green's functions. For example,

$$v_2(\vec{q}) = 1 + UkT \sum_{i\omega} \sum_p \sum_{m,m'} G_{m,m'}(\vec{p}, i\omega) \times G_{m',m}(\vec{p} + \vec{q}, i\omega) , \tag{17}$$

$$v_2(\vec{q}) = 1 - U\chi_0(\vec{q}) , \tag{18}$$

where $\chi_0(q)$ is the noninteracting susceptibility. Similar expressions can be written down for higher-order vertices. The fourth-order vertex is illustrated in Fig. 4.

The correlation functions (11) can be computed by means of a diagrammatic expansion in which the quadratic term in (16) is taken as the unperturbed Hamiltonian.³¹ The unperturbed and full propagators are

$$D_0(\vec{q}) = 2 \langle \xi(\vec{q}) \xi(-\vec{q}) \rangle_0 = \frac{1}{1 - U\chi_0(q)} , \tag{19}$$

$$D(\vec{q}) = 2 \langle \xi(\vec{q}) \xi(-\vec{q}) \rangle . \tag{20}$$

A self-energy is defined as

$$D^{-1}(\vec{q}) = D_0^{-1}(\vec{q}) - U\Sigma(\vec{q}) \tag{21}$$

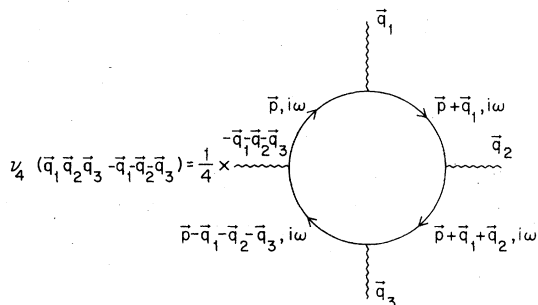


FIG. 4. Fourth-order spin-fluctuation vertex. The meaning of the symbols is explained in the text.

in terms of which the susceptibility is

$$\chi(\vec{q}) = 2 \frac{\phi(\vec{q})}{1 - U\phi(\vec{q})} , \tag{22}$$

where

$$\phi(\vec{q}) = \chi_0(\vec{q}) + \Sigma(\vec{q}) . \tag{23}$$

Some low-order diagrams for $\Sigma(q)$ are shown in Fig. 5. A wiggly line represents an unperturbed propagator. Each vertex carries a factor of $(UkT)^{1/2}$. Internal momenta, frequency, and orbital indices have to be summed over.

In a Hartree-like approximation³¹ only those diagrams that contain a single closed loop of electron lines are retained and wiggly lines are replaced by full propagators. Figures 5(a) to 5(d) are examples of diagrams included in this approximation whereas diagrams like Figs. 5(e) and 5(f) are neglected.

Further progress in the evaluation of the self-energy can be made by examining the momentum dependence of the dressed fluctuation propagator. Comparison of Eqs. (11) and (19) shows that

$$D(\vec{q}) = \frac{1}{1 - U\phi(\vec{q})} . \tag{24}$$

The q dependence of $\phi(q)$ is qualitatively similar to that of $\chi_0(q)$.³⁴ Within the model Hamiltonian used here $\phi(q)$ has a large maximum near the edge of the Brillouin zone ($\vec{q} = \vec{Q}$) and a much smaller one at $\vec{q} = 0$. Away from these points $\phi(q)$ decays rapidly. Thus, the leading contribution to a given graph for the self-energy comes from nearly antiferromagnetic and nearly ferromagnetic spin fluctuations. One can treat these fluctuations exactly while approximating the effects of those at other wave vectors by evaluating each diagram as if the only momenta transferred to the electron lines were $\vec{q} = 0$ and \vec{Q} . In practice

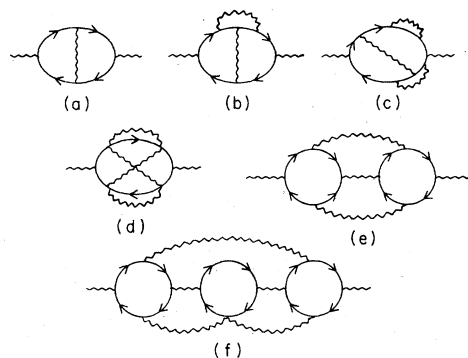


FIG. 5. Some contributions to the spin-fluctuation self-energy. Diagrams (a) to (d) are retained in the approximation used in this paper.

this means that wiggly lines are replaced by either of

$$\begin{aligned}\sigma_0^2 &= UkT \frac{1}{2N} \sum_p D(p) \\ &= UkT \frac{1}{2N} \sum_p \frac{1}{1 - U\phi(p)},\end{aligned}\quad (25)$$

$$\begin{aligned}\sigma_s^2 &= UkT \frac{1}{2N} \sum_p D(p+Q) \\ &= UkT \frac{1}{2N} \sum_p \frac{1}{1 - U\phi(p+Q)},\end{aligned}\quad (26)$$

depending on whether the momentum they carry is near $\bar{q}=0$ or \bar{Q} . The diagrams simplified in this way are exactly those for the average susceptibility of a system of noninteracting electrons moving in the presence of random uniform and staggered magnetic fields h_u and h_s . These fields have Gaussian distributions with widths given by (25) and (26), respectively. Explicitly,

$$\phi(\bar{q}) = \langle \chi_0(\bar{q}, h_f(\bar{x})) \rangle_{h_f}, \quad (27)$$

where

$$h_f(\bar{x}) = h_u + h_s \cos(\bar{Q} \cdot \bar{x}). \quad (28)$$

The amplitudes h_u and h_s are distributed according to

$$P(h_{u,s}) = \frac{1}{\sqrt{2\pi}\sigma_{u,s}} \exp\left[-\frac{h_{u,s}^2}{2\sigma_s^2}\right]. \quad (29)$$

Rather than attempting to solve the system of self-consistent equations (25)–(29) for the q -dependent $\phi(q)$, it is convenient to parametrize its decay away from the center and the edge of the Brillouin zone in the form

$$\phi(\bar{q}) = \phi(0) \left[1 - \left(\frac{q}{q_u} \right)^2 \right], \quad (30)$$

$$\phi(\bar{q} + \bar{Q}) = \phi(\bar{Q}) \left[1 - \left(\frac{q}{q_s} \right)^2 \right], \quad (31)$$

valid for small values of q . The cutoff momenta q_u and q_s are taken as parameters to be determined by comparison of calculated and observed quantities. This approximation is made in order to simplify the computations and is of no consequence for the physics of the results.

The uniform and staggered susceptibilities may now be obtained from (22) and (25) to (31). With the definitions $\lambda_u = U\chi(0)$ and $\lambda_s = U\chi(\bar{Q})$ one finds the following system of self-consistent equa-

tions:

$$\frac{\lambda_u}{1 + \lambda_u} = U \langle \chi_0(0, h_f(\bar{x})) \rangle_{h_f}, \quad (32)$$

$$\frac{\lambda_s}{1 + \lambda_s} = U \langle \chi_0(\bar{Q}, h_f(\bar{x})) \rangle_{h_f}, \quad (33)$$

$$\sigma_{u,s}^2 = \frac{UkT}{4\pi^2} q_{u,s}^3 \frac{1 + \lambda_{u,s}}{\lambda_{u,s}} \left[1 - \frac{\tan^{-1}(\lambda_{u,s}^{1/2})}{\lambda_{u,s}^{1/2}} \right]. \quad (34)$$

The solutions of this system used in conjunction with (30) and (31) give the temperature-dependent bulk nonlocal susceptibility.

The same procedure can be extended to the ordered phase after shifting the variables of integration to take into account the nonzero average value of the magnetization density. The latter can be evaluated with the result

$$M(\bar{x}) = \langle M_0(\bar{x}, h_f'(\bar{x})) \rangle_{h_f}, \quad (35)$$

where

$$h_f'(\bar{x}) = h_u + h_s \cos(\bar{Q} \cdot \bar{x}) + \frac{U}{2} M(\bar{x}). \quad (36)$$

Here, M_0 is the equilibrium value of the magnetization density of a system of noninteracting electrons in the magnetic field (36). The last term on the right-hand side of Eq. (36) is the Hartree-Fock field. The first two terms represent the effect of the thermal fluctuations. As $T \rightarrow 0$ the widths of the distributions of h_u and h_s vanish. Thus, at $T=0$ the random fields can be neglected completely and Eq. (35) reduces to the Hartree-Fock result, Eq. (4).

B. Surface fluctuations

The decoupling that leads to Eq. (15) follows from Eq. (9) if all local fields except the one at site i are neglected in the evaluation of $G_i(E)$. Intersite coupling modifies the on-site propagators in two ways. If the system is in the ordered phase the electrons see an average spin-dependent potential. This can be taken into account by adding to H_0 the Hartree-Fock term. At nonzero temperature spin reversals occur with a finite probability. Their effect is to add a random component to the spin-dependent potential. In the spirit of effective-medium theory³⁵ one can approximately take the latter into account in a calcula-

tion of $G(E)$ by treating the local field at site i and the average potential exactly but replacing the random potential on other sites by an energy-dependent effective potential to be chosen in a self-consistent way.³⁶ Given the fact that surface fluctuations are much stronger than bulk fluctuations it seems

reasonable to assume that the effective potential is localized at the surface. Since the random potential is local it is further assumed that the effective potential is also local. With these approximations, the effective Hamiltonian to be used in the calculation of $G_{im,im}(E)$ is

$$H_{\text{eff}}(E) = H_0 + \sum_{j,m,s} s \frac{U}{2} M_j c_{jms}^+ c_{jms} + \sum_{j,m,s'} \sigma_{jm}^s(E) c_{jms}^+ c_{jms} \quad (37)$$

where M_j is the average magnetization at site j and the last sum extends over surface sites only. From (37) and (9) the local free energy is obtained

$$F(\Delta_i) = \frac{\Delta_i^2}{U} + \int \frac{dE}{\pi} f(E) \sum_{s,m} \text{Im} \ln \{ 1 + [s\Delta_i - [s\bar{\Delta}_i + \sigma_{im}^s(E)] \langle G_{im}^s(E) \rangle] \} \quad (38)$$

where

$$\langle G(E) \rangle = \frac{1}{E - H_{\text{eff}}(E)} \quad (39)$$

At the surface $F(\Delta)$ has two minima at Δ^\pm which are the solutions of

$$2\Delta_i^\pm = -U \int \frac{dE}{\pi} f(E) \sum_{s,m} s \text{Im} \frac{\langle G_{im}^s(E) \rangle}{1 + [s\Delta_i^\pm - s\bar{\Delta}_i + \sigma_{im}^s(E)] \langle G_{im}^s(E) \rangle} \quad (40)$$

It will be seen later that these minima are very sharp. Thus, the saddle-point configurations are those in which the surface field takes the values Δ^\pm with probabilities

$$p_i^\pm = \frac{1}{1 + \exp \pm [F(\Delta_i^+) - F(\Delta_i^-)]} \quad (41)$$

The simplest choice for the effective potential in this problem is given by the CP (coherent potential) approximation, which gives the self-energy³⁶

$$\sigma_{im}^s(E) = -[s\Delta_i^+ - s\bar{\Delta}_i + \sigma_{im}^s(E)][s\Delta_i^- - s\bar{\Delta}_i + \sigma_{im}^s(E)] \langle G_{im}^s(E) \rangle \quad (42)$$

From Eqs. (40) and (41) the surface magnetization is found

$$M_i = \frac{2}{U} (p_i^+ \Delta_i^+ + p_i^- \Delta_i^-) \quad (43)$$

Equations (37) to (43) depend on the magnetization on layers below the surface through the second term on the right-hand side of (37). To evaluate the magnetization profile (35) and (36) must be generalized to include the effect of the surface. The presence of the latter modifies the results of Sec. III A in two ways. The Hartree-Fock term in Eq. (36) now contains the true self-consistent magnetization profile, and the fields h_u and h_s become position dependent. Assuming that h_u and h_s retain their bulk values right up to the surface, (35) and (36) can be expanded in powers of the deviation of the true pro-

file from the one appropriate for an infinite system. Keeping terms up to third order the equation for the profile becomes

$$\Delta M(l) = U \sum_{l'} \phi(l, l') \Delta M(l') + \frac{\alpha}{2} \Delta M^2(l) + \frac{\gamma}{3} \Delta M^3(l) + \dots \quad (44)$$

where

$$\Delta M(l) = M(l) - M_\infty(l) \quad (45)$$

Above T_N $M_\infty(l)$ vanishes. Below the Néel temperature it is the spin-density-wave profile. In Eq. (44) nonlocal terms of higher than first order have been neglected. The nonlocal kernel in (44) is the Fourier

transform of the $q_{\parallel}=0$ component of (29),

$$\phi(l, l') = \sum_{q_z} \phi(q_{\parallel}=0, q_z) \exp\left[iq_z(l-l')\frac{a}{2}\right]. \quad (46)$$

The coefficients of the second- and third-order terms are given by averages over the fluctuating fields of derivatives of the local magnetization with respect to

the local field

$$\alpha = \frac{U^2}{4} \left\langle \frac{d^2}{dh_l^2} M_l(h_l) \right\rangle, \quad (47)$$

$$\gamma = \frac{U^3}{16} \left\langle \frac{d^3}{dh_l^3} M_l(h_l) \right\rangle. \quad (48)$$

After some straightforward algebra Eq. (44) can be cast in the form

$$\coth\left(\frac{q_s}{2\sqrt{\lambda_s}}\right) \Delta M(l) + \frac{1}{2} \operatorname{csch}\left(\frac{q_s}{2\sqrt{\lambda_s}}\right) [\Delta M(l+1) + \Delta M(l-1)] = \frac{q_s(1+\lambda_s)}{4\sqrt{\lambda_s}} \left[\frac{\alpha}{2} \Delta M^2(l) + \frac{\gamma}{3} \Delta M^3(l) \right], \quad (49)$$

where λ_s is the dimensionless staggered susceptibility obtained from (32)–(34). In deriving this equation only nearly antiferromagnetic fluctuations have been included because, as it will be seen later, they are dominant over the whole temperature range of interest. The nonlinear difference equation (49) can be numerically solved subject to the boundary conditions

$$\lim_{l \rightarrow \infty} M(l) = M_{\infty}(l), \quad (50)$$

$$M(l=0) = M_s, \quad (51)$$

where M_s is the surface magnetization. At a given temperature the profile is completely determined by the surface magnetization and the system (34) to (43) can be solved for the latter.

At very low temperature only one solution of (40) survives, namely, the one corresponding to the lowest free energy. It is not hard to see that in this case the system of equations reduces to the Hartree-Fock condition for the surface magnetization.

IV. RESULTS OF NUMERICAL CALCULATIONS

In order to solve the self-consistent equations (32)–(34) and (38)–(42) one must compute susceptibilities and Green's functions for electrons moving in the presence of arbitrary magnetic fields. Due to the number of integrals that must be evaluated numerically and the requirement of self-consistency, these quantities must be evaluated a large number of times. The perturbative version of the continued-fraction expansion technique²⁴ is an efficient way of performing these calculations. In this method, for a given choice of unperturbed Hamiltonian, the recursion coefficients $[a_n, b_n]$ ²⁴ are expanded in a series of powers of the perturbation which, in this case, is the sum of the fluctuating and average magnetic fields, and the CPA self-energy. In the present problem all the perturbations are local and homogeneous in the directions parallel to the surface. The continued-

fraction coefficients for a site on layer l are expanded as

$$a_n(l) = a_n^0(l) + \sum_{l'} a_n^1(l, l') V(l') + \sum_{l', l''} a_n^2(l, l', l'') V(l') V(l'') + \dots \quad (52)$$

with a similar expression for $b_n(l)$. The expansion coefficients $a_n^1(l, l')$ and $a_n^2(l, l', l'')$ need to be calculated only once in the process of generating the set $[a_n^0(l), b_n^0(l)]$. The susceptibilities, derivatives of the local magnetization with respect to various magnetic fields, are related to derivatives of the Green's functions. From Eq. (52) and the standard recursion relations for $G(E)$ one can derive recursion relations for the latter. The results reported here were obtained by truncating Eq. (52) after the second-order term and terminating the continued fractions in the usual way²⁴ after the eighth level. This involves working with a cluster of about 2600 atoms.

Figure 6 shows the bulk staggered and uniform magnetic susceptibilities as functions of temperature as computed from Eqs. (32)–(34). The Néel temperature is determined as that at which the staggered susceptibility diverges. In order to reproduce the experimental value of T_N the cutoff q_s must be taken as about a quarter of the distance between opposite faces of the Brillouin zone in the [001] direction. For simplicity the same value was taken for q_u .

It can be seen from Fig. 6 that χ_s is strongly temperature dependent. It varies as $(T - T_N)^{-2}$ near T_N and obeys a Curie-Weiss law at higher temperatures. The behavior near T_N is a result of using a self-consistent approximation for the spin-fluctuation self-energy. In contrast, the uniform field susceptibility is featureless and varies slowly with temperature. The equilibrium-staggered magnetization, shown in Fig. 7, shows the expected mean-field behavior, vanishing at T_N as $(T_N - T)^{1/2}$ and saturating at low temperature. The fact that the Néel temperature determined from the susceptibility and the

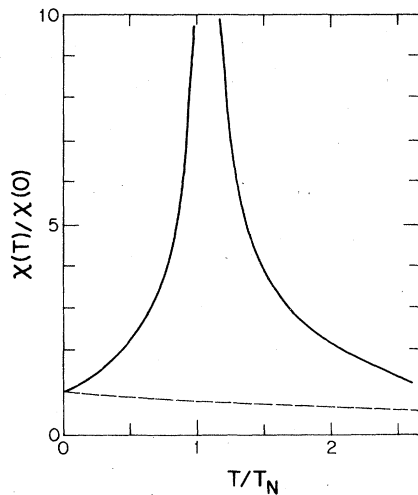


FIG. 6. Staggered (solid line) and uniform (dashed line) susceptibilities for bulk chromium.

magnetization coincide indicates that the approximations used above and below T_N are consistent with each other.

The condition for the existence of a surface phase transition is that Eqs. (38)–(42) have a nonvanishing solution. The existence of such a solution depends on the strength of the coupling between the surface spins to those on layers below. This coupling is most simply characterized by the rate of decay of the magnetization to its bulk value. For infinitesimal surface magnetization Eq. (49) has an exponentially decaying solution $\Delta M(l) \sim \exp(-\Lambda l)$ where Λ is a function of the temperature. The stability of an ordered surface depends on the value of Λ . Although the present model allows one to calculate this quantity, it is useful to regard it temporarily as a free parameter. It was found that for large Λ , weak coupling, a fer-

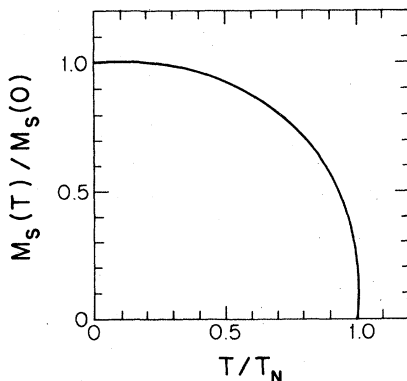


FIG. 7. Equilibrium staggered magnetization of bulk chromium as a function of temperature.

romagnetic surface is unstable at all temperatures and antiferromagnetic ordering within the surface plane becomes favored, implying that the effective interaction between surface spins is antiferromagnetic. For small Λ , strong coupling, a ferromagnetic surface becomes stable at some temperature above T_N . Using the computed values of Λ it is found that surface ferromagnetism is stable for temperatures below $T_s = 900$ K.

Figure 8 shows the probability distribution of local band splittings at different temperatures. Two equivalent maxima appear at and above T_s , corresponding to the local magnetization pointing "up" or "down." At lower temperatures the symmetry is broken and one of the states becomes favored. Near the maxima the distributions are quite sharp, which justifies the use of the saddle-point method in the calculation of the thermodynamic quantities. The average size of the local band splitting, $\langle \Delta^2 \rangle^{1/2}$, increases slightly as the temperature decreases. In the ground state it is about 10% larger than in the paramagnetic phase. This temperature dependence is a self-energy effect resulting from stronger spin-disorder scattering at higher temperatures.

The spontaneous surface magnetization is shown in Fig. 9. It vanishes at T_s in mean-field fashion and saturates quite rapidly. Its value at T_N is essentially the surface ground-state moment. The magnetization profile, computed from Eq. (49), is plotted at different temperatures in Fig. 10. The magnetization alternates in sign from layer to layer. For convenience, only the magnitude of the magnetization is shown in the figure. The fact that the curves are smooth is a result of the parametrization in Eqs. (30) and (31).

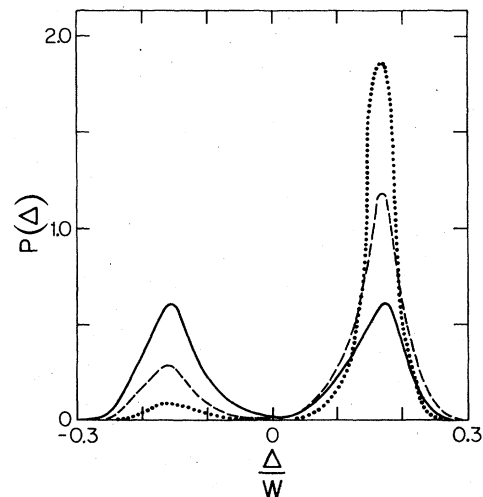


FIG. 8. Probability distributions of the surface local band splitting at $T = T_s$ (solid line), $T = 0.5T_s$ (dashed line), and $T = T_N$ (dotted line).

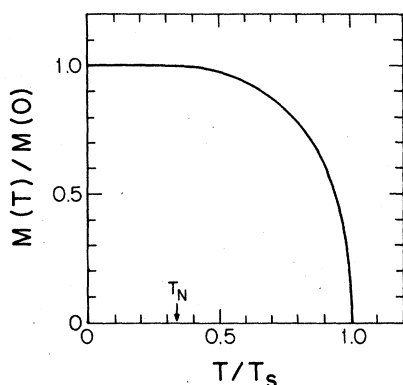


FIG. 9. Spontaneous surface magnetization as a function of temperature. The arrow points at the bulk Néel temperature.

If the full \bar{q} dependence of $\phi(\bar{q})$ is retained the shape of the curves is modified by quantum oscillations as described by other authors.¹⁻⁴ However, this effect is important only at very low temperature. At higher temperatures the oscillations are suppressed by thermal broadening. After an initial decay that is controlled by the nonlinear terms in Eq. (49) the magnetization decays exponentially both above and below T_N . Since the bulk correlation length is shorter, the decay is faster in the ordered phase. As expected, at T_N the decay is very slow reflecting the divergence of the bulk correlation length.

Below T_s the total magnetization per surface atom is finite and localized near the surface because the configuration of the spins deep in the bulk is antiferromagnetic in nature. The temperature dependence of the total magnetization is shown in Fig. 11. This peculiar shape, with a maximum at T_N , results from the fact that the total bulk polarization, opposite to the surface moment, decreases as the temperature is

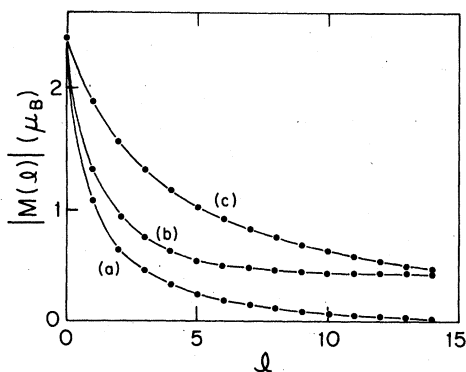


FIG. 10. Magnetization profile at different temperatures: (a) $T = 1.5 T_N$, (b) $T = 0.5 T_N$, (c) $T = T_N$. The solid curve is a guide to the eye. Notice that only the magnitude of M is plotted.

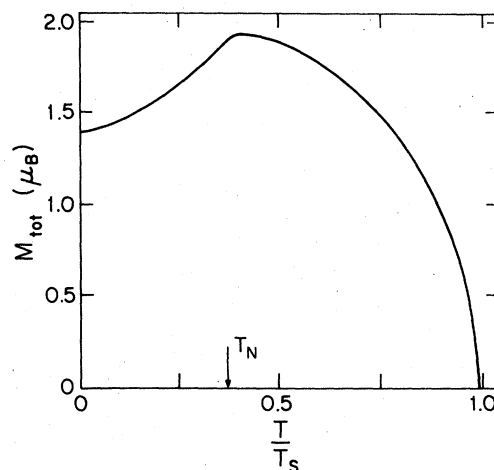


FIG. 11. Total magnetization per surface atom as a function of temperature.

raised towards T_N . This produces an increase of the total magnetic moment.

These results agree qualitatively with the available experimental evidence. The persistence of surface ordering above T_N was observed in small particles of chromium.¹⁸ The experimental critical temperature (~ 800 K) is of the same order of magnitude as the one predicted here. The maximum at T_N in the total magnetization was also observed although the theory predicts an effect substantially smaller than what was observed experimentally. The magnetization curve is also consistent with the result of the optical experiments¹⁹ performed in the vicinity of T_N . Direct observation of magnetic moments was reported in work with ultrathin films of chromium confined between thicker films of gold.¹¹ Although the geometry in this case is very different from the one studied here, it is tempting to suggest that the basic mechanism is the same in both cases. Further understanding of the role of surface local moments may be gained by following the surface peaks as a function of temperature in photoemission experiments. If the picture of surface local moments holds, one expects to see exchange-split surface bands with the exchange splitting persisting above the critical temperature, in analogy with what is observed in the case of bulk ferromagnetic metals.³⁷

V. SUMMARY AND CONCLUDING REMARKS

The bulk and surface magnetic properties of chromium have been studied within a spin-fluctuation model. The bulk shows the behavior expected for an antiferromagnetic metal with no local-moment formation. In contrast, large localized moments form at the surface. These moments interact antiferromagnetically and, in the absence of coupling

to the bulk, these interactions would favor surface antiferromagnetism. However, coupling to the bulk is strong and stabilizes a ferromagnetic surface at temperatures quite far above T_N . The temperature-dependent bulk antiferromagnetic fluctuations produce polarization effects that give to the total magnetization a characteristic temperature dependence.

Due to the complexity of the problem it was necessary to make several approximations. In the calculation of the surface fluctuation effects an alloy analogy was used which overestimates the effect of disorder and neglects the presence of short-range correlations. Although at the cost of considerable computational effort, the latter can be taken into account by adapting to the case of the surface the methods already developed for the bulk.³⁸ More serious is the neglect of the effect of the surface on the amplitude of the fluctuating fields on the layers below it. It would be desirable to include these effects in a self-consistent way for, in that case, one would get a more accurate picture of the decay of the magnetization on the layers immediately below the surface which are the most relevant for the interpretation of surface-

sensitive experiments. Unfortunately, this task seems extremely difficult at this stage. In the case of the (001) surface the electronic properties, which ultimately determine the magnitude of the fluctuation effects, are bulklike already at the second layer. This suggests that the surface effect on the bulk fluctuating fields may be not too large. Similar methods can be applied to problems involving thin films of transition metals and other systems with confined geometry that are of current experimental interest. These and other related topics are presently under consideration.

ACKNOWLEDGMENTS

It is a pleasure to thank G. B. Blanchet for many useful suggestions concerning the manuscript, and T. C. Lubensky for bringing Ref. 18 to the author's attention. Thanks are also due to P. Soven for a critical reading of the manuscript. This work was supported by the NSF-MRL program under Grant No. DMR-7923647.

- ¹J. P. Muscat, M. T. Beal-Monod, D. M. Newns, and D. Spanjard, *Phys. Rev. B* **11**, 1437 (1975).
- ²S. C. Ying, L. M. Kahn, and M. T. Beal-Monod, *Solid State Commun.* **18**, 359 (1976).
- ³S. C. Ying and L. M. Kahn, *Surf. Sci.* **67**, 278 (1977).
- ⁴E. Zaremba and A. Griffin, *Can. J. Phys.* **53**, 891 (1975).
- ⁵G. Bergman, *Phys. Rev. Lett.* **41**, 264 (1978).
- ⁶R. J. Celotta, D. T. Pierce, G. C. Wang, S. D. Baden, and G. P. Felcher, *Phys. Rev. Lett.* **43**, 728 (1979).
- ⁷C. Rau, *Bull. Am. Phys. Soc.* **25**, 234 (1980).
- ⁸A. H. Owens, J. Tyson, G. Bayreuther, and J. C. Walker, in *Proceedings of the 26th Conference on Magnetism and Magnetic Materials*, Dallas (unpublished).
- ⁹H. Akoh and A. Tasaki, *J. Phys. Soc. Jpn.* **42**, 791 (1981).
- ¹⁰M. B. Brodsky and A. J. Freeman, *Phys. Rev. Lett.* **45**, 133 (1980).
- ¹¹M. Brodsky, in *Proceedings of the 26th Annual Conference on Magnetism and Magnetic Materials* (unpublished).
- ¹²A. I. Ahonen *et al.*, *J. Phys. (Paris) Colloq.* **37**, C9-1665 (1976); and *Phys. Rev. Lett.* **41**, 494 (1978).
- ¹³C. S. Wang and A. J. Freeman, *Phys. Rev. B* **19**, 793 (1979).
- ¹⁴C. S. Wang and A. J. Freeman, *J. Magn. Magn. Mater.* **15-18**, 869 (1980).
- ¹⁵D. R. Gempel and S. C. Ying, *Phys. Rev. Lett.* **45**, 1018 (1980).
- ¹⁶M. T. Beal-Monod and S. Doniach, *J. Low Temp. Phys.* **28**, 175 (1977).
- ¹⁷H. Takayama, K. P. Bohnen, and P. Fulde, *Phys. Rev. B* **14**, 2287 (1976).
- ¹⁸S. Matsuo and I. Nishida, *J. Phys. Soc. Jpn.* **49**, 1005 (1980).
- ¹⁹P. E. Ferguson, *J. Appl. Phys.* **49**, 2203 (1978).
- ²⁰Y. Teraoka and J. Kanamori, in *Transition Metals*, edited by M. J. G. Lee (Institute of Physics, Bristol and London, 1978), p. 588.
- ²¹J. Hubbard, *Phys. Rev. B* **19**, 2626 (1979).
- ²²G. Allan, *Surf. Sci.* **74**, 79 (1978).
- ²³D. G. Dempsey, L. Kleinman, and E. Caruther, *Phys. Rev. B* **14**, 279 (1976).
- ²⁴R. Haydock, in *Solid State Physics*, edited by H. Ehrenreich, F. Seitz, and D. Turnbull (Academic, New York, 1980), Vol. 35, p. 216.
- ²⁵J. E. Inglesfield, *Surf. Sci.* **76**, 379 (1978).
- ²⁶G. P. Kerker, K. M. Ho, and M. L. Cohen, *Phys. Rev. B* **18**, 5473 (1978).
- ²⁷S. A. Werner, A. S. Arrott, and H. Kendrick, *Phys. Rev.* **155**, 528 (1967).
- ²⁸C. R. Fincher, G. Shirane, and S. A. Werner, *Phys. Rev. Lett.* **43**, 1441 (1979).
- ²⁹G. Allan, *Phys. Rev. B* **19**, 4774 (1979).
- ³⁰J. Hubbard, *Phys. Rev. Lett.* **3**, 77 (1959).
- ³¹J. A. Hertz and M. A. Klenin, *Phys. Rev. B* **10**, 1084 (1974).
- ³²W. E. Evanson, J. R. Schrieffer, and S. Q. Wang, *J. Appl. Phys.* **41**, 1199 (1970).
- ³³F. W. Wiegel, *Phys. Rep.* **16C**, 57 (1975).
- ³⁴H. Hasegawa and T. Moriya, *J. Phys. Soc. Jpn.* **36**, 1542 (1974).
- ³⁵H. Hasegawa, *J. Phys. Soc. Jpn.* **46**, 1504 (1979).
- ³⁶P. Soven, *Phys. Rev.* **156**, 747 (1968).
- ³⁷D. E. Eastman, F. J. Himpsel, and J. A. Knapp, *Phys. Rev. Lett.* **40**, 1514 (1978).
- ³⁸V. Korenman, J. L. Murray, and R. E. Prange, *Phys. Rev. B* **16**, 4032 (1977).